Modelling of a Solar Thermal Reactor for Hydrogen Generation

Jürgen Dersch   Andreas Mathijssen   Martin Roeb   Christian Sattler

Deutsches Zentrum für Luft- und Raumfahrt e.V. (DLR)

Institute of Technical Thermodynamics, Solar Research

51170 Köln, Germany

juergen.dersch@dlr.de   andreas@mathijssen.de   martin.roeb@dlr.de   christian.sattler@dlr.de

Abstract

The transient thermal behavior of a solar thermal reactor for hydrogen generation has been modeled using Modelica/Dymola. The model is used to predict temperatures and reaction rates inside the reactor which is operated alternating between two temperature levels. The purpose of this reactor is the production of hydrogen as a future carbon free fuel using exclusively regenerative energy resources.

First results are promising and the model may be used to explain experimental observations from the operation as well as for theoretical studies.

Keywords: solar, hydrogen, chemical reaction, heat conduction

1   Introduction

Hydrogen generated from renewable energy sources has the potential to become an important energy carrier for the future, particularly for mobile applications. Beside the well known path of using electrical energy from renewables for electrolysis, the solar heat may be used directly for water splitting without the additional step of electricity generation. Whereas direct thermal water splitting needs temperatures above 2500 K, several multi-step thermo-chemical processes are known, enabling the hydrogen generation at temperatures which are controllable by today's technical equipment. One of these thermo-chemical processes is currently under investigation in the HYDROSOL-2 project funded by the EC [1]. A two-step water splitting process has been developed using mixed iron-oxides on a porous ceramic structure in a reactor heated directly by solar radiation. The reactor is operated with alternating reaction conditions, in particular with two alternating temperature levels of about 1073 K and 1350 K respectively. Experimental results from a small scale lab reactor are available which prove the general feasi-

bility of the process and the "cycleability" of the redox materials. A scale-up of the technology aiming at the demonstration in a 100kW-scale is in progress.

From this short description and the fact that solar radiation varies with daytime and cloud coverage, it is evident that the operation of this reactor is highly dynamical. Therefore a mathematical tool is necessary in order to model the reactor for theoretical studies and scale-up.

2   Description of the process and the experimental setup

The experimental and theoretical work is focused on a thermo-chemical cycle using materials that can act as effective water splitters at moderate temperatures in a two-step reaction scheme. The overall reaction may be described by the following steps which are conducted successively at different temperature levels:

$$MO_{reduced} + H_2O \rightarrow MO_{oxidized} + H_2 \qquad (1)$$

$$MO_{oxidized} \rightarrow MO_{reduced} + O_2 \qquad (2)$$
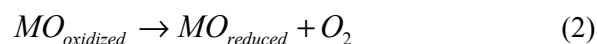
The metal oxides (MO) used in this particular reaction are ion oxides doped with other divalent metals (Zn, Ni, Mn). The basic idea is to employ an innovative monolithic solar reactor for the production of hydrogen from the splitting of steam using solar energy, by combining a refractory ceramic thin-wall, multi-channeled (honeycomb) support structure optimized to absorb solar radiation and develop sufficiently high temperatures, with a redox pair system suitable for the performance of water dissociation and at the same time suitable for regeneration at these temperatures. With this concept complete operation of the whole process (water splitting and redox material regeneration) can be achieved by a single solar energy converter.

Figure 1 shows a cross section of the experimental reactor used for the first experiments in the solar fur-

nace at DLR, Cologne. The outer diameter of the housing is 0.43 m and the diameter of the porous silicon carbide structure carrying the ion oxides is 0.144 m. The front side is covered by a quartz glass window for the concentrated sunlight admission. The concentrated sunlight is provided by a mirror system capable for concentrations up to 5000 suns.
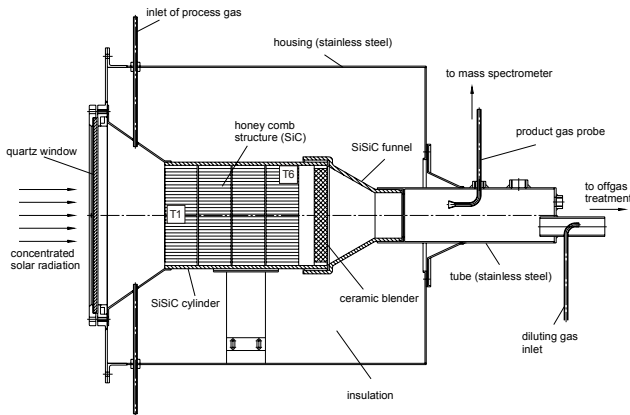
Figure 1: Cross section of the laboratory scale reactor for solar thermal hydrogen production

Typical input power for this experimental setup was between 2000 and 3000W. The input gases (N_2 and H_2O) are fed via four small tubes radially distributed over the reactor circumference. The entrance for these gases is on the right hand side of Figure 1 and the flow direction is form right to left. Behind the SiC structure, a ceramic blender is used, to achieve an optimal mixing and then the gases are leaving the reactor to the product gas analysis and off-gas treatment.

Figure 2: Photo of the laboratory scale reactor for solar thermal hydrogen production

The typical operation of this reactor may be described by the following steps:

1. Preheating of the cold reactor with concentrated solar radiation up to 1073 K.

2. Steam admission and production of hydrogen at 1073 K.

3. Increasing the solar thermal input in order to reach the higher temperature level of 1350 K.

4. Regeneration period at this temperature level. During this period the reactor is flushed with nitrogen.

5. Reduction of the solar thermal input to come down to the low temperature level of 1073 K

Steps 2-5 are repeated consecutively until the end of the experiment. Experimental setup with two reactors of this type, each one in a different step, has also been tested in order to get a continuous hydrogen production.

3   Model approach

An overall model has been set up for this reactor in Dymola using partial models from the standard library Modelica 2.2 in combination with the Modelica_Fluid library and additional adapted or newly developed models. The main purpose of this first model approach is the simulation of the thermal behavior of the reactor. Reaction kinetics are considered by simple preliminary approaches since quantitative experimental data on reaction velocities are not yet available.

Figure 3 shows a screenshot of the overall model. The model is 2-dimensional due to the rotational symmetry of the reactor. From this figure, it becomes obvious, that most of the icons used here are from the Modelica 2.2 library. This is also valid for most of the associated models, but some of them have been modified in order to meet the special requirements. The only model used without any modifications is the Modelica.Blocks.Sources.CombiTimeTable for input data of ambient temperature and solar power input. These values are available from measurements in the solar furnace and they are used as input data for the simulations.

The input model MassFlowSource is a descendant of CombiTimeTable too, but with some additional code to allow for input flows with different units (like kg/s or l/h) and multiple output flows in SI units. PrescribedTemperature, Convection, FeedPump, IdealMixer and Sink are made from standard Modelica models with the extensions of distributed connectors and multi-component mass flows. The reactor, the insulation and the solar heat input distribution are new models and further details are given below.
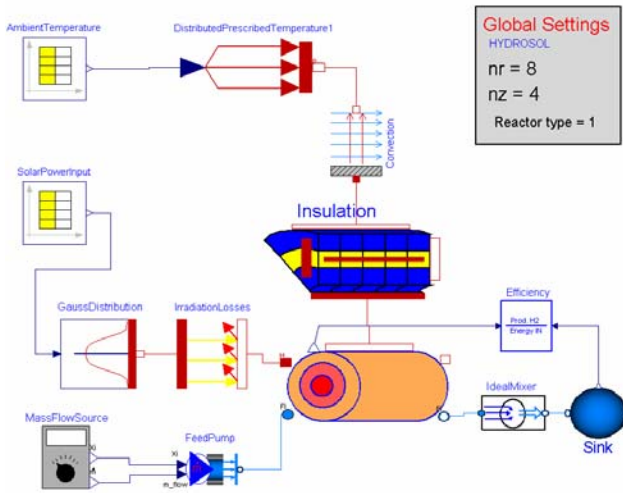
Figure 3: Screenshot of the overall model used for the simulation of the laboratory scale reactor for solar hydrogen generation

The spatial distribution of solar radiation input is not constant throughout the aperture, it shows a Gaussian-like shape with a peak in the centre and considerably lower values towards the rim. Measurements of the flux distribution at the reactor entrance are available as well as the integral value of the solar power input during the experiments. The object called "GaussDistribution" in Figure 3 is used to distribute the total input power among the individual rings of the reactor front surface. The shape of the power distribution is approximated by the equation:

$$P(r) = P_{total} \left[y_0 + \frac{a_0}{w\sqrt{0.5\pi}} \exp\left(-2\left(\frac{r}{w}\right)^2 \right) \right] \quad (3)$$

Measured values of the input flux distribution at nominal power are shown in Figure 4 in comparison to this approximation. Although the measured distribution is not exactly symmetrical, this assumption was made for the model in order to use a 2-dimensional model and restrict the number of equations.

The object IrradiationLosses in Figure 3 is used to model the thermal losses due to absorption and re-radiation through the quartz glass window at the front side of the reactor. The result is a net power input to the reactor depending on the actual surface temperature.

The ceramic monolith inside the reactor as well as the insulation and the housing are modeled as concentric circular rings build up from several slices in axial direction (Figure 5). Mass and energy balances

are set up using the finite volume method as described in [2].
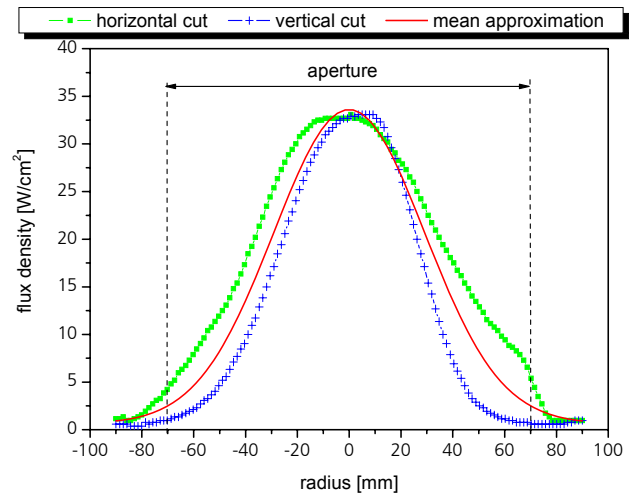
Figure 4: Measured and approximated flux density at the reactor entrance.

Pressure gradients are neglected in this model. They are low enough to neglect an influence on the chemical reactions but the authors are well aware that there may occur instabilities influencing the local gas flow and thereby the temperature distribution within the ceramic monolith [3]. Therefore these local pressure drops may be incorporated into a more advanced future model.
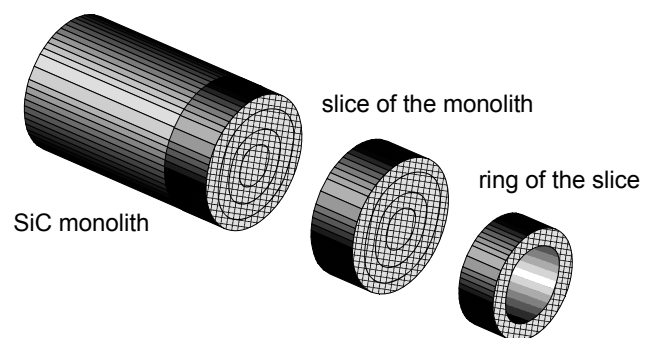
Figure 5: Balance volumes used for the model of the solid SiC monolith

The cylindrical ceramic monolith as the main component of the solar hydrogen reactor is modeled by three major objects:

1. the "solid"-object representing the SiC matrix with the task of absorbing the radiation at the front surface and providing an even temperature distribution by heat conduction,

2. the "fluid"-object representing the gas channels with square cross sections to allow a gas flow through the reactor,

3. and the "coating"-object for the reactive layer, which is located at the inner surface of the SiC matrix.

The latter object may be considered as intermediate layer between the solid and the fluid object. Its mass balance accounts for accumulation or release of oxygen depending on the operating conditions. The fluid object does not consider any mass accumulation and concentrations of the gaseous species are assumed to be constant within each control volume. Transport resistance between fluid and coating is neglected as well. Since the coating itself has a very small mass and heat capacity, the thermal inertia is represented solely by the SiC matrix.

The solid object is based on the differential equation for 2-dimensional heat transfer in cylinder coordinates:

$$\rho\,c\,\frac{\partial T}{\partial t} = \frac{1}{r}\frac{\partial}{\partial r}\left(r\lambda\frac{\partial T}{\partial r}\right) + \frac{\partial}{\partial z}\left(\lambda\frac{\partial T}{\partial z}\right) + \phi \qquad (4)$$

A central difference scheme was applied to approximate the spatial partial derivatives. The effective thermal conductivity of the SiC honeycomb structure is not the same for the radial and the longitudinal direction since the solid walls show different thickness. The effective values are calculated according to cross section fraction covered by the solid material. For the radial direction the equation reads:

$$\lambda_r = \frac{A_{r,solid}}{A_{r,total}}\lambda \qquad (5)$$

The fluid object contains an instance of Modelica.Media.IdealGases.Common.MixtureGasNasa representing a mixture of N_2, H_2O, H_2 and O_2. This Modelica package provides all fluid properties needed for the simulation.

At present, the knowledge about reaction kinetics is only marginal and therefore the reaction rate is calculated by a preliminary equation based on investigations of Tsuji et al. [4]. The experimental investigation of reaction rates of Tsuji et al. have been carried out in the temperature range between 250 and 350°C, which is much lower than the operating temperature range of the solar reactor.

$$(3+\delta)Fe_3O_4 + 4\,\delta\,H_2 \underset{v_2}{\overset{v_1}{\rightleftharpoons}} 3Fe_{3+\delta}O_4 + 4\,\delta\,H_2O$$

$$(6)$$
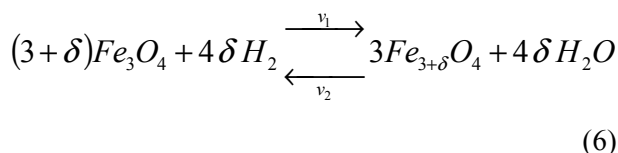
According to [4] the overall reaction rate for the water splitting is:

$$v_S = v_2 - v_1 = k_2\,\delta^{0.95}\,p_{H_2O}^{0.45} - k_1\,p_{H_2}^{1.1} \qquad (7)$$

with

$$k_1 = 5.345e-12\exp\left(-\frac{63.8}{RT}\right) \qquad (8)$$

and

$$k_2 = 0.03634\exp\left(-\frac{25.5}{RT}\right) \qquad (9)$$

For the reverse regeneration reaction

$$(3+\delta)Fe_3O_4 \overset{v_3}{\rightarrow} 3\,Fe_{3+\delta}O_4 + 2\,\delta\,O_2 \qquad (10)$$
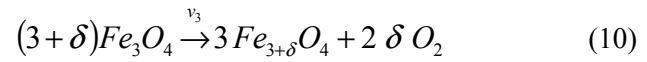
The velocity is calculated from

$$v_3 = k_3\,\frac{m_{O_2,stored}}{V_{react}} \qquad (11)$$

$$k_3 = 2.1e8\,\exp\left(-\frac{225}{RT}\right) \qquad (12)$$

Activation energy and frequency factor in Eq. (10) are estimated from the experimental observations that a considerable reaction rate does not take place beyond 1200 K and the time period needed for a complete regeneration is about 20 minutes. It should be emphasized, that these reaction rates are only first estimates and further investigations are necessary in order to get more reliable data about these reactions. The solar reactor is not suitable for this kind of experiments because the number of uncertain parameters is quite high. They should be carried out under well defined and almost constant conditions, e.g. in a differential reactor.

The temperature distribution inside the reactor, the total product mass flow rate, and the efficiency of the reactor are important results from this model.

4 Simulation results

The first experiments with the solar reactor were performed without any hydrogen production in order to investigate the thermal behavior of the plant. Figure 6 shows simulation results in comparison to measured data from one of these first experiments. Inside the ceramic monolith only one thermocouple is mounted for temperature measurement. It is located at the center near the front side where the feed gases

and the solar radiation are entering the monolith (see Figure 1).

The matching of simulated and measured temperatures is fairly good, a conclusion which is also valid for other experiments. The remaining differences are due to model simplifications and also due to uncertainties in the available physical properties, e.g. the thermal conductivity of SiC at elevated temperatures, which is not exactly known since it depends on the material and also on the processing of the monolith.
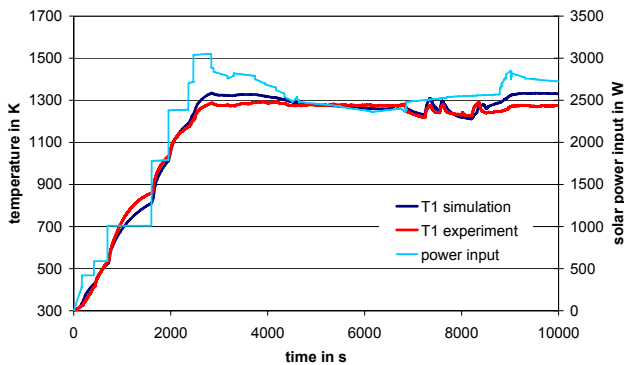
Figure 6: Comparison of measured and calculated temperature in the center of the reactor for a start-up.

The model was also used to investigate the sensitivity with regard to the reactor length. Figure 7 shows the results of this study. Here two different lengths of the ceramic reactor element have been simulated: 5 cm (the actual length used in the laboratory reactor) and 10 cm. Beside the length and the number of axial balance volumes all input parameters are identical. In Figure 7 the temperature along the center axis is drawn for steady state conditions. The temperature curve for the 10 cm monolith is not affected by the number of discrete elements (4 or 8). The shorter monolith shows a lower temperature towards the gas exit (right hand side). This result was unexpected because the heat input is at l=0 and with increasing distance the temperature should decrease from a first feeling. Heat transfer and temperature compensation between solid and gas are the main reason for the temperature decrease along the axis. The gas feed is cold compared to the temperature of the SiC and the temperature balancing needs about 4 cm independently of the reactor length.

The remaining temperature decrease of gas and solid is due to losses caused by radial heat conduction. Due to the extended heat transfer area between gas and solid for the longer monolith, the radial losses are smaller than for the shorter type. This behavior is supported by the different effective solid heat conductivity in axial and in radial direction. Due to the macroscopic structure the conductivity in axial direc-

tion is 1.72 times of the conductivity in radial direction.
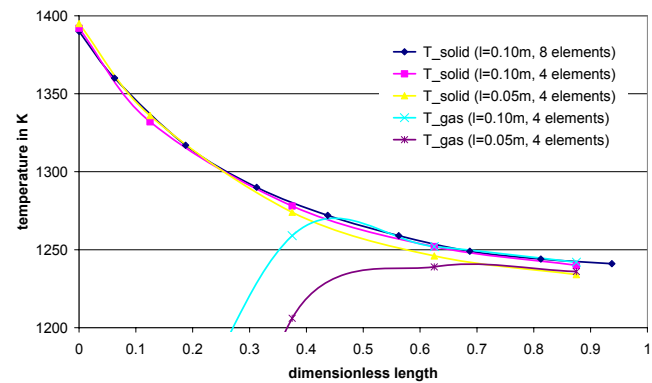
Figure 7: Study on the dependency of reactor length and number of axial discrete volume elements (steady state conditions)

Since the temperature difference at the exit for both lengths is not very large (about 8 K) its impact on the reaction rate may be neglected compared to other model uncertainties. From Figure 7 it is also obvious, that the gas and solid temperatures are equalized at the exit of the monolith for both lengths. Nevertheless, a doubling of the monolith length means also a doubling of the reactive surface, which could be an advantage for the chemical reaction because the available reactive coating is twice as for the short monolith.

The solar reactor shown in Figure 1 has been redesigned and currently a dual reactor concept is used for continuous hydrogen production. This type has two reaction chambers; one can be operated in production mode while the other one is in regeneration mode (Figure 8). After a certain time period the power input and the gas feed are shifted and the operation mode is inverted. The shape and the dimensions of the SiC monolith are the same as for the original reactor. Experimental data with hydrogen production are available from this setup.
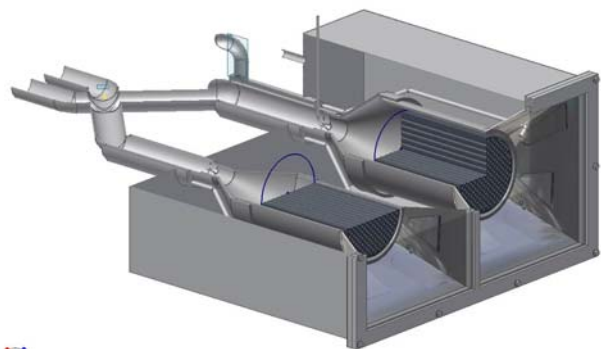
Figure 8: Drawing of the dual reactor for solar hydrogen production

The main difference between both reactors from the model point of view is the rectangular shape of the insulation and the outer shell. This would break the rotational symmetry and account for a 3-dimensional model. Nevertheless the 2-dimensional approach has been used for the simulation in order to limit the calculation time. Since the rectangular geometry is only used for the outer shell, this approximation seems to be still acceptable. Furthermore the current knowledge about the chemical reaction allows only a qualitative comparison of simulation and experiment concerning the hydrogen production rate. Consequently the main purpose of the model is not the prediction of hydrogen production rate but the dynamical thermal analysis of the reactor since the spatial and temporal temperature distribution inside the ceramic monolith is of great importance for the reactor performance.

For this qualitative comparison the input data was simplified and smoothened because particularly the solar power shows many fluctuations and the experimental dataset has a temporal resolution of 5 seconds. According to the Modelica concept, this would lead to many events and thus to unacceptable simulation times. Figure 9 shows the simplified power input and two calculated temperatures. T1 is the temperature in the center of the monolith near the front side and T6 at the outer rim of the monolith near the back side.
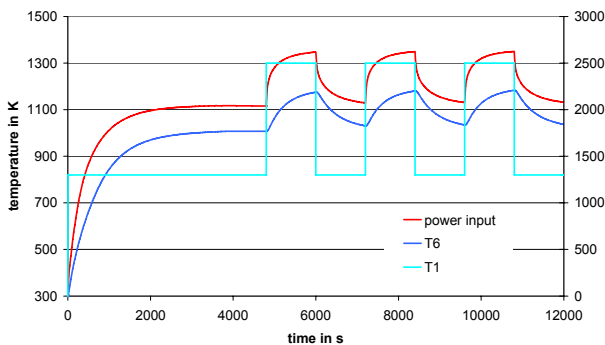
Figure 9: Solar power input and calculated temperatures of a reactor startup and 3 cycles of hydrogen production and regeneration. (see Figure 1 for the position of T1 and T6)

The first hour was used to heat up the whole installation by solar radiation and the steam admission starts at t=3600s. At the same time the hydrogen production starts with a peak mass flow rate, which is decreasing during the next 1200s of the experiment (Figure 10). At t=4800s the steam input is stopped, the solar power input is increased immediately to heat up the reactor and the regeneration period starts. At t=6000s the hydrogen production starts again, but with a lower initial rate than the first time. This periodic operation is repeated two more times. From Figure 9 it is obvious, that the temperature difference between T1 and T6 is about 100 – 170K, which concurrently represents the largest temperature difference inside the monolith.

An acceptable matching between experiment and simulation was reached by adjusting the reaction rate parameters k_1 and k_2, although the reaction rates are highly temperature dependent and more reliable kinetic data is urgently desired.
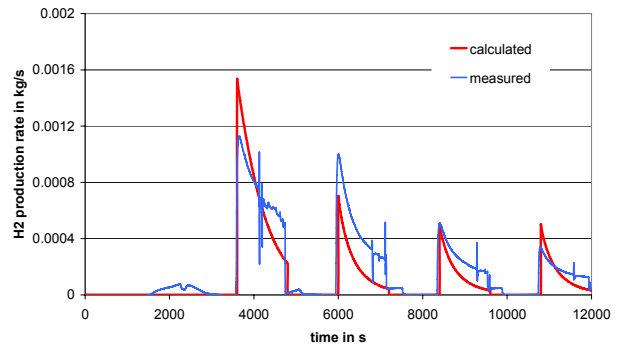
Figure 10: Comparison of calculated and measured hydrogen production rates

The temperature difference between T1 and T6 in Figure 9 may be used to explain the decreasing initial hydrogen production rate, which is presumably caused by large temperature gradients inside the ceramic structure. These temperature gradients are preventing a complete regeneration of the reactive layer since a certain temperature level is necessary for this step.

Figure 11 shows the absolute mass of available ferrite, which is the figure determining the potential of hydrogen production since the oxygen is captured by these ferrite molecules. Three curves are shown, the total amount of ferrite, the amount in the center and at the outer rim of the monolith.

The amount of available ferrite for the new monolith starts at a high initial level, decreases during the first hydrogen production period (3600 – 4800s) and increases again during the regeneration period (4800 – 6000s). The regeneration is incomplete and the next cycle starts at a lower initial peak ferrite concentration compared to the first cycle. The simulation results are demonstrating that the regeneration reaches an almost constant peak level at the second regeneration cycle (8400s) because the same value (0.06 mol) is achieved for the following cycle. From Figure 11 it is also obvious, that the incomplete regeneration is caused mainly by the outer areas of the monolith, which are not hot enough for regeneration. This lower temperature is caused by the lower solar power

input towards the rim and the radial heat losses at this area.
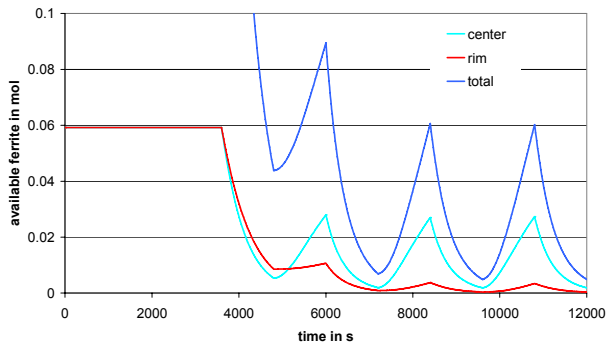
Figure 11: Calculated values of available ferrite for the center part, the outer part and the whole monolith during the periodic operation

5   Conclusions

The Modelica language has been used to set up a model for a solar heated hydrogen generation reactor and to simulate the dynamic behavior of the reactor. First results are promising and the model may be used to explain the decreasing reaction rates, which have been observed during the experiments. The main purpose of the model is the prediction of the thermal dynamics of this reactor rather than the prediction of the hydrogen production rate. Nevertheless heat production and heat consumption are combined with the reactions and therefore the proper calculation of the reaction rates is important for the heat balances.

Model developments as well as experimental investigations are continued, in order to get a deeper insight into this interesting path of solar energy utilization. Next steps are model refinements as well as the set up of a structured library and simulations of an up-scaled plant.

This project was the first experience of the authors using Modelica/Dymola though they have been using other modeling languages (Smile [5]) in the past. The initial orientation period in Dymola/Modelica was rather short and successful working was possible after an acceptable time. Due to the complex matter, general knowledge about dynamical models and the continuous working with the software is an advantage for the person performing the work.

Acknowledgement

Symbols

Symbol	Description	Units
A	area	m²
a_0	coefficient of the solar power input distribution	-
c	specific heat capacity	J/(kg K)
k_1	reaction rate constant for water recombination	mol/(dm³ s Pa$^{1.1}$)
k_2	reaction rate constant for water splitting	mol/(dm³ s Pa$^{0.45}$)
k_3	reaction rate constant for regeneration	mol/(kg s)
P	power input	W
p	partial pressure	Pa
R	gas constant	kJ/(mol K)
r	radius, coordinate in radial direction	m
T	temperature	K
t	time	s
v	reaction velocity	mol/(dm³s)
w	standard deviation of the power distribution	-
y_0	coefficient of the solar power input distribution	-
z	coordinate in axial direction	m
δ	amount of excess cations	-
φ	internal heat source	W/m³
λ	thermal conductivity	W/(m K)
ρ	density	kg/m³

References

[1]   Roeb, M., Monnerie, N., Schmitz, M., Sattler, C., Konstandopoulos, A., Agrafiotis, C., Zaspalis, V.T., Nalbandian, L., Steele, A., Stobbe, P.: Thermo-chemical production of Hydrogen from Water by Metal Oxides Fixed on Ceramic Substrates, Proceedings of the 16th World Hydrogen Energy Conference, Lyon, France, June 13-16, 2006.

[2]   Elmqvist H., Tummescheit H., Otter M.: Object-Oriented Modeling of Thermo-Fluid Systems, Modelica 2003, Sweden, November 3-4, 2003.

[3]   Buck R., Massenstrom-Instabilitäten bei volumetrischen Receiver-Reaktoren, VDI-Verlag, Düsseldorf, 2000.

[4]   Tsuji M., Togawa T., Wada Y., Sano T., Tamaura, Y., Kinetic Study of the Formation of Cation-excess Magnetite, J. Chem. Soc. Faraday Trans. 1995 , 91(10), 1533-1538.

[5]   Jochum P. , Kloas M. The Dynamic Simulation Environment Smile. In Tsatsaronis Ed., Second Biennal European Conference on System Design & Analysis (1994), pp. 53-56. ASME